**Oncogene (1998) 16,** 1065–1075
© 1998 Stockton Press All rights reserved 0950–9232/98 $12.00

# Functional capabilities of molecular network components controlling the mammalian G1/S cell cycle phase transition

Kurt W Kohn

*Laboratory of Molecular Pharmacology, Division of Basic Sciences, National Cancer Institute, National Institutes of Health, Bethesda, Maryland 20892, USA*

**The molecular interactions implicated in the mammalian G1/S cell cycle phase transition comprise a highly non-linear network which can produce seemingly paradoxical results and make intuitive interpretations unreliable. A new approach to this problem is presented, consisting of (1) a convention of unambiguous reaction diagrams, (2) a convenient computer simulation method, and (3) a quasi-evolutionary method of probing the functional capabilities of simplified components of the network. Simulations were carried out for a sequence of hypothetical primordial systems, beginning with the simplest plausibly functional system. The complexity of the system was then increased in small steps, such that functionality was added at each step. The results suggested new functional concepts: (1) Rb-family proteins could store E2F in a manner analogous to the way a condenser stores electric charge, and, upon phosphorylation, release a large wave of active E2F; (2) excessive or premature cyclin-dependent kinase activities could paradoxically impair E2F activity during the G1/S transition period. The results show how network simulations, carried out by means of the methods described, can assist in the design and interpretation of experiments probing the control of the G1/S phase transition.**

**Keywords:** molecular reaction network modeling; molecular reaction diagrams; computer simulation of reaction networks; cell cycle models; G1/S phase transition; E2F; retinoblastoma protein

## Introduction

The molecular steps implicated in eukaryotic cell cycle regulation have a daunting complexity that challenges our ability to comprehend their integrated functions (Kohn and Dimitrov, 1997). The difficulty arises not only from the large number of molecular interactions, but more importantly from their non-linear character. Unlike classical networks of metabolic pathways which may encompass a large number of reactions, regulatory networks of even modest size present special difficulties because (1) the enzymes are often substrates of other enzymes (e.g. kinases, phosphatases, and proteases), (2) some of the molecular species are transcription factors that influence the synthesis rates of other species in the same system, and (3) the enzymes and regulatory proteins often combine to form functional or non-functional multimers. These non-linearities can make it difficult to interpret experiments, for example on the effects of altered gene expression or of specific inhibitors. One is apt to encounter seemingly paradoxical results. Moreover, regulatory networks often contain closed loops, and it can then be confusing to ask whether a particular step is 'upstream' or 'downstream' of another. Under these circumstances, intuition becomes unreliable and simulation may become necessary.

Previously reported cell cycle simulations generally focused on autonomous cycling behavior (Goldbeter, 1991, 1996; Hyver and Le Guyader, 1990; Kauffman and Willie, 1975; Norel and Agur, 1991; Novak and Tyson, 1993b, 1995; Obeyesekere *et al*., 1995; Tyson, 1991; Tyson *et al*., 1996), as exemplified by observations on amphibian egg extracts (Felix *et al*., 1990; Hutchison *et al*., 1987; Murray and Kirschner, 1989; Murray *et al*., 1989). The previous models included assumptions at the differential equations level, invoked in order to produce cycling behavior, which confer to these models a 'macroworld' aspect (Kholodenko and Westerhoff, 1995). The models studied in the present work do not involve autonomous cycling and focus instead on a single cell cycle phase transition. Moreover, the models in the present work are defined entirely in terms of molecular interactions and therefore qualify as pure 'microworld' models (Kholodenko and Westerhoff, 1995).

Recently accumulated data on mammalian cells indicates that progress of these cells through cycle is governed by checkpoints (Hartwell and Kastan, 1994; Hartwell and Weinert, 1989; Murray, 1992; O'Connor, 1997; Elledge, 1996). A checkpoint is an inhibitory signal that prevents the onset of a subsequent cell cycle event until a preceding cell cycle process has been completed. Checkpoints may be viewed as signals from cell structures, i.e. from outside the cell cycle regulatory network itself, that prevent autonomous cycling. Cell cycle control thereby becomes linked to the entities being controlled.

Several checkpoints have been extensively studied in mammalian cells. (1) The initiation of mitosis remains in check (subject to delay) until no more unreplicated or damaged DNA is detected (Fingert *et al*., 1986, 1988; Lau and Pardee, 1982; Lock, 1992; Muschel *et al*., 1991; O'Connor, 1997; O'Connor *et al*., 1993, 1994; Tobey, 1975; Wang *et al*., 1996). A model of the transition leading to mitosis has been analysed in detail (Novak and Tyson, 1993a). (2) The transition from metaphase to anaphase remains in check until no more chromosomes remain unaligned on the mitotic spindle (recently reviewed by Wells (1996) and by Rudner and Murray (1996)). (3) Most relevant to the current work is the control event that commits cells to prepare for

Correspondence: KW Kohn
Received 24 July 1997; revised 30 September 1997; accepted 30 September 1997

and begin DNA replication, i.e. to make the transition from G1 phase to S phase (Bartek *et al*., 1996; Campisi *et al*., 1982; Dou *et al*., 1993; Pardee, 1988). Pardee (1989) assigned the term 'restriction point' to this event, which is thought to control the proliferation of normal and cancer cells. An analogous control has been defined in yeast where it is called 'start' (Nasmyth, 1993) and has been modeled from the standpoint of phase portraits of a system of differential equations (Tyson *et al*., 1995). The commitment of mammalian cells to S phase remains in check while metabolite deficiencies or unrepaired DNA damage are detected (reviewed by Bartek *et al*. (1996)).

The present study focuses on regulatory events occurring as mammalian cells prepare for and enter S phase. Rather than attempting to simulate the entire set of reactions known to participate in this process, we take what might be termed a 'quasi-evolutionary' approach. We begin with the smallest subset of reactions that could provide rudimentary functional capability and then add components in small successive steps such that each increment to the system adds potentially useful functionality.

We begin with the E2F transcription factors which can be viewed as a main output of the network that controls entry into S phase. Members of the E2F family regulate the transcription of genes for a variety of products required by the DNA replication machinery (see summary table in Hurford *et al*. (1997)), and ectopic expression of E2F1 suffices to drive quiescent cells into S phase (Johnson *et al*., 1993; Qin *et al*., 1994). Although E2F comprises a family of heterodimers, the present simulations will consider E2F as a single monomeric species.

Members of the E2F family are known to bind to members of the retinoblastoma (Rb) gene family which include p107 and p130 (for recent reviews on the interactions of Rb and E2F family proteins, see Sherr (1996) and Bartek *et al*. (1996)). The current simulations however will include only one Rb family member. Binding of Rb-family proteins inhibits the transcriptional activity of a number of E2F-regulated genes (Hurford *et al*. (1997) and references cited therein). A family of cyclin-dependent kinases (cdk) hyperphosphorylates Rb in the complex with E2F, thereby destabilizing the complex and causing the release of active E2F. Ectopic expression of Rb can arrest cells in G1, and co-expression of E2F1 can overcome this arrest and allow cells to enter S-phase (Qin *et al*., 1995). The cdks are regulated by binding to a cyclin, which is required for kinase activity, and by phosphorylations which can be either stimulatory or inhibitory. Cdk4 (and its close relative cdk6) are the preferred partners of cyclin D, while cdk2 can pair with cyclin E or cyclin A. As cells progress towards and into S phase, there is a sequential activation of cyclin D, cyclin E, and cyclin A functions (reviewed by Sherr (1996)). We will consider the first two and defer the latter. Kohn and Dimitrov (1997) have previously carried out simulations of a similar model by means of a system of differential equations.

A premise tested in the current work is that a quasi-evolutionary sequence of simulations of hypothetical primordial systems (hps) can provide functional insights useful for the interpretation of experiments and for guidance of experimental inquiry. This report establishes procedures for this type of investigation and describes the results of a first quasi-evolutionary path in the G1/S cell cycle control network. The results suggest some previously unsuspected relationships that could be probed experimentally. In addition, a general method is described for the production of unambiguous reaction diagrams that define the input to a molecular network simulation program.

## Results

### *Reaction diagrams*

A notation for explicit reaction diagrams was devised that uniquely defines the modeled reaction steps and that can be translated into an input file for a simulation program. Some important features of this type of diagram are (1) each monomer species is depicted only once; (2) each molecular complex is represented essentially as a unique point or node; (3) unique symbols are used to represent (a) binding between molecular species, (b) stoichiometric conversion of one molecular species to another, (c) stimulation by one molecular species of the production of another, and (d) modification of a monomer species by covalent addition of small molecules. The symbols are defined and illustrated in Figure 1).

This method of representing reaction diagrams has several advantages once familiarity with the diagram conventions is attained. (1) The diagrams unambiguously define the topology of the network. (2) Since each molecular species essentially appears only once in

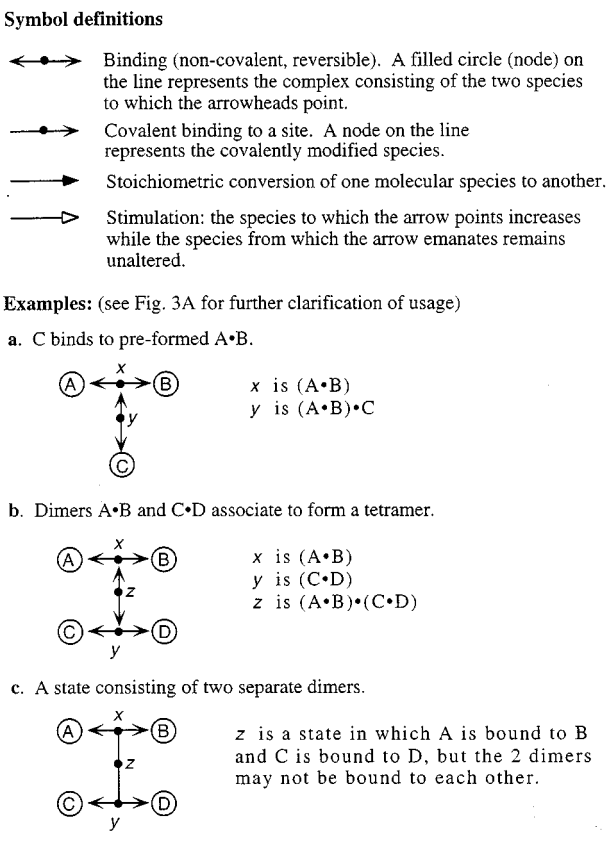


**Figure 1** Definition of symbols used in explicit reaction diagrams

the diagram, it is easy to trace all of the reactions involving a given species. (3) A reaction diagram can readily and essentially automatically be translated into a reaction file that serves as input to the computer program that carries out the simulations, and it is not necessary to write out the differential equations explicitly. (4) It then becomes relatively easy to modify the network and to carry out simulations for a series of modified networks.

The starting point for the selection of symbols was the representation of multi-subunit complexes by means of a line with barbed arrowheads at both ends. A 'line' can change direction but cannot branch. Binding lines imply both association and dissociation of the two connected molecular species. Since a molecular species can itself be a complex, the number of subunits in a represented complex can be built up indefinitely. In selecting the preferred assembly paths leading to a complex, care must be taken not to omit paths that may dominate certain situations. A complex is represented by a small filled circle or 'node' on a binding line; for clarity, two or more nodes may be placed on the same binding line and all represent exactly the same complex. A variant of this notation is sometimes useful to represent by means of a single node a set of separate molecular species; this is accomplished simply by omitting the barbed arrowheads (Figure 1, example c). The utility of these conventions will become clearer in the context of the reaction diagrams in subsequent Figures.

### *Hps A1: an Rb-like factor regulates the delay time for onset of E2F accumulation*

Our starting point, hps A1, is comprised of an E2F transcription factor, its production and degradation, and its inhibition by binding to an Rb-like protein (Figure 2). In hps A1, E2F is synthesized at a constant rate and degraded subject to a rate-limiting component of a proteolytic process. Recent observations indicate that E2F is degraded by the ubiquitin-proteasome pathway (Hateboer *et al*., 1996; Hofmann *et al*., 1996); hence the rate-limiting step could be an enzyme in the ubiquitination sequence. E2F binds irreversibly to Rb, forming an inactive complex. (Inclusion of a slow reversal rate did not materially alter the results). When bound to Rb, E2F is protected against degradation (Hateboer *et al*., 1996; Hofmann *et al*., 1996). The simulations in Figure 2b show, in the absence of Rb, the expected rapid steady-state accumulation of free E2F. In the presence of Rb, the onset of E2F accumulation is delayed until Rb nears saturation. This simple model suggests how a primitive Rb-like factor could control the time of onset of DNA replication. In this way a primitive cell could delay replication until some degree of growth has occurred.

### *Hps A2: an Rb-like factor generates an E2F wave in response to a cdk-like kinase*

The next step in the quasi-evolutionary sequence will be to add a cdk-like kinase that phosphorylates Rb in Rb-E2F complex and thereby causes the complex to dissociate. Extensive evidence indicates that hyperphosphorylation of Rb allows cells to progress to S phase (reviewed by Weinberg 1995). The resulting network

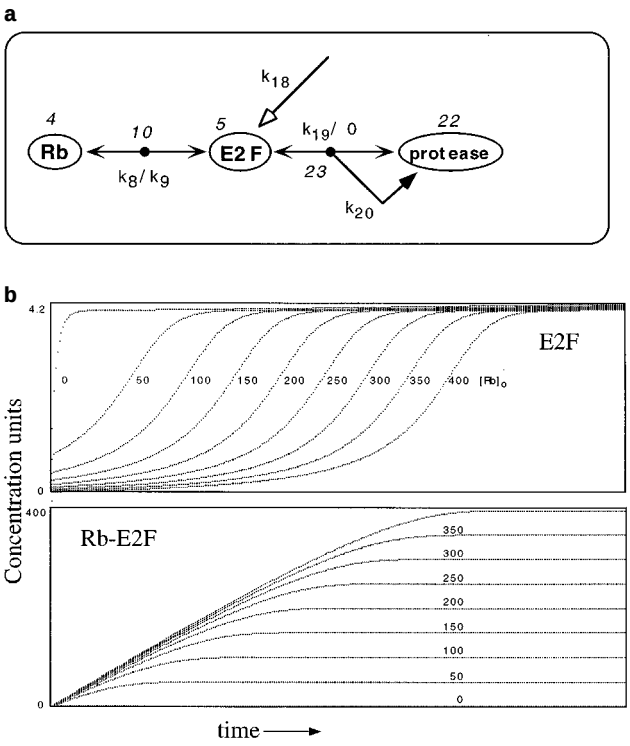


**Figure 2** Hps A1: a simple system in which Rb regulates the delay time for onset of E2F accumulation. (**a**) Reaction diagram. An E2F-like factor (species 5) is synthesized at a constant rate (k18). E2F binds rapidly to Rb to form E2F-Rb (species 10). E2F is degraded by a specific (e.g. ubiquitin-dependent) protease system, the essential steps of which are binding of E2F to a component of the protease system (species 22) to form intermediate 23 and conversion of 23 to 22 (E2F disappears while 22 is regenerated). (**b**) Simulation. For the indicated initial Rb concentrations $[Rb]_o$, the curves show concentration versus time for E2F (upper panel) and Rb-E2F (lower panel). In the absence of Rb, E2F rapidly achieves a steady-state concentration. Rb binds E2F until saturated, thereby delaying the onset of accumulation of free E2F. Parameter settings: $k_8 = 0.1$, $k_9 = 0$, $k_{18} = 8$, $k_{19} = 4$, $k_{20} = 16$, $[E2F]_o = 0$, $[protease]_o = 1$, $[Rb]_o$ as marked. (k18 refers to the stimulated production of E2F from a unit precursor whose concentration remains perpetually equal to 1). The horizontal axis extends from 0–96 time units

(hps A2) is diagrammed in Figure 3a and described in the legend. Although Rb may be phosphorylated equally well whether free or bound to E2F, only the latter case was included in order to keep these initial models as simple as possible. (Both phosphorylation paths will be included in the network sequence, hps B).

The simulation in Figure 3b shows the development of a delayed wave of free E2F. During the first phase, newly synthesized E2F binds rapidly to Rb. As E2F synthesis proceeds, free Rb falls and Rb-P rises nearly linearly. During this process, however, Rb-E2F accumulates (temporarily, up to 51.7 concentration units in this simulation). Therefore, Rb is depleted before all Rb has been phosphorylated (time interval between vertical dashed lines A and B in Figure 3b). When free Rb is nearly depleted (at vertical dashed line A), E2F begins to rise due to the release of E2F upon phosphorylation of the Rb in the Rb-E2F complex (free Rb no longer being available to re-bind the freed E2F). When Rb-E2F is depleted (vertical dashed line B), free E2F declines and settles to a steady-state balance between synthesis and degradation.

This model suggests how an Rb-like factor together with a cdk-like kinase can control the appearance of a wave of E2F activity. Rb functions to store up E2F as a condenser stores electric charge. Thus Rb family members, which are generally considered to function as E2F inhibitors, may also serve to generate a large wave of E2F activity.

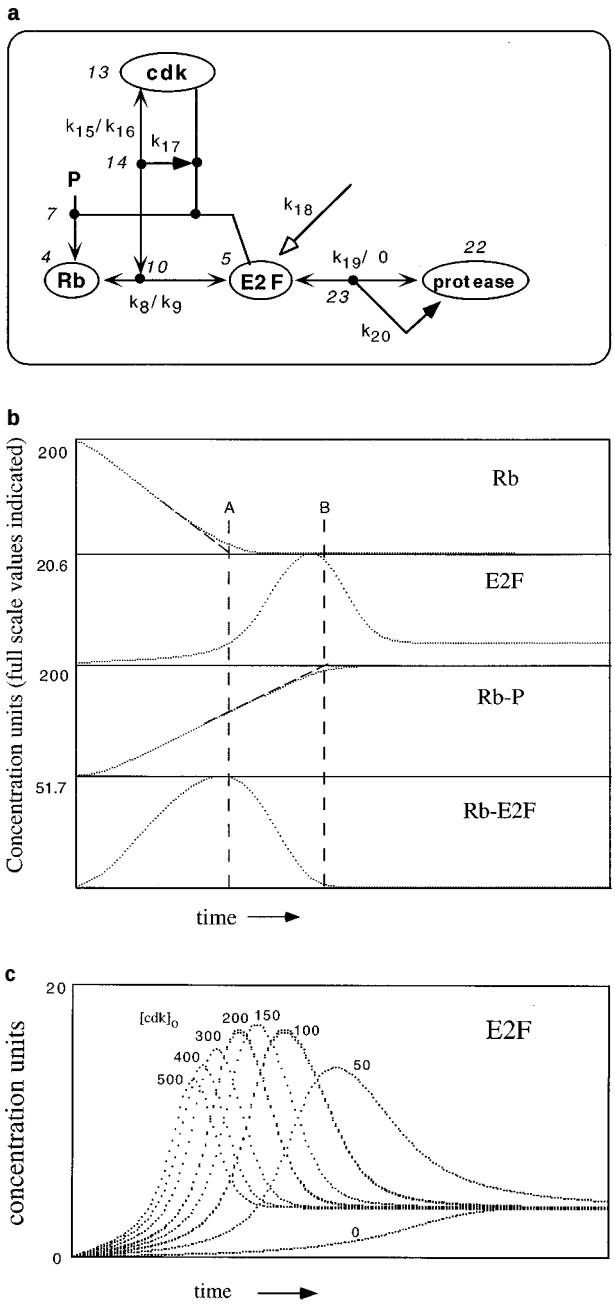


**Figure 3** Hps A2: a system in which Rb generates an E2F wave in response to a kinase (cdk) that phosphorylates Rb. (**a**) Reaction diagram. Added to hps A1 is a cdk-like kinase that phosphorylates Rb in Rb-E2F complex and thereby causes the complex to dissociate. Cdk binds reversibly to Rb-E2F, forming complex 14 (association constant $k_{15}$, dissociation constant $k_{16}$). Species 14 decomposes to form Rb-P (species 7), E2F, and cdk (rate constant $k_{17}$); note the use of nodes on non-arrowed connecting lines to indicate the dissociated reaction products (see Figure 1, example c). (**b**) Simulation showing how a wave of E2F is generated. Parameters: $k_{15}=k_{16}=0.2$, $k_{17}=0.4$; $[Rb]_o=200$, $[cdk]_o=20$; other conditions are as in hps A1. The vertical dashed lines indicate the times when nearly all of the Rb has been depleted (line A) and when nearly all of the Rb has been hyperphosphorylated (line B). Horizontal axis runs from 0–96 time units. (**c**) Simulations showing the E2F responses to the indicated initial cdk concentrations [cdk]o, with $k_{15}=0.002$, $k_{17}=5$, other parameters as in **b**

Another characteristic of hps A2 is seen when simulations are carried out with different initial cdk concentrations (Figure 3c). There is an optimum cdk concentration that generates the greatest amplitude of E2F response. Excessive cdk concentrations diminish the E2F response, because Rb becomes phosphorylated so rapidly that less E2F can be stored as Rb-E2F complex. Although the magnitude of this effect was limited in this simulation, it will be seen in the hps B series (for example, Figure 6b) that the effect can become much larger. This behavior suggests that excessive expression of cdk activity could produce a seemingly paradoxical impairment of S phase response.

### *Hps A3: addition of cyclin E-cdk2 dimerization and E2F-dependent expression of cyclin E gene provides a sharp trigger for expression of active cyclin E-cdk2*

In hps A2, cdk was taken to be a monomolecular species of given initial concentration that was neither synthesized nor degraded, and the cyclin partner was ignored. We now add a cyclin. We select cyclin E and its partner, cdk2, because this activity appears to be a central part of the G1/S regulatory machinery (Lukas *et al*. (1997) and references cited therein).

In hps A3, cyclinE-cdk2 is the entity that phosphorylates Rb (see diagram in Figure 4a). We must also address the regulation of cyclin E and cdk2, i.e., their production, modification, and degradation. Cdk2 activity is affected by both stimulatory and inhibitory phosphorylations. However, because of the complexity of this control, we will at this time consider this aspect of the system only in a superficial manner. The cyclin E gene contains E2F elements in its promoter and appears to be regulated at least in part by E2F (Botz *et al*., 1996; DeGregori *et al*., 1995; Ohtani *et al*., 1995); we therefore add this feedback loop in hps A3 (see reaction diagram Figure 4a). In regard to degradation or inactivation of cyclin E, recent evidence indicates that cyclin E is inactivated by autophosphorylation which causes the cyclinE-cdk2 complex to dissociate (Won and Reed, 1996); we therefore include this reaction in hps A3 (Figure 4a). (Phosphorylated cyclin E may then be degraded, but, since it is taken to be an inactive end-product, its actual degradation need not be added to the scheme).

Figure 4b (top) shows the dependence of the wave of free E2F on $k_{17}$. This rate constant governs the cyclinE-cdk2-catalysed phosphorylation of Rb and can be viewed as a surrogate for phosphorylation state of cdk2. As $k_{17}$ is increased, the size of the wave of free E2F first increases and then decreases. Here again excessive cdk activity impaired the E2F response.

The maximum accumulation of Rb-E2F decreases steadily as $k_{17}$ is increased (Figure 4b, middle). The response of cyclinE-cdk2 shows a sharp onset which occurs earlier, but is smaller, when $k_{17}$ is larger (Figure 4b, bottom). It is interesting to note here that a later response is a larger response.

Figure 4c (top) shows the dependence of the wave of free E2F on cyclin E gene dosage (or number of E2F-responsive promoter elements on E2F genes). We see that excessive cyclin E gene dosage, like excessive cdk activity, can reduce the size of the E2F response. (As

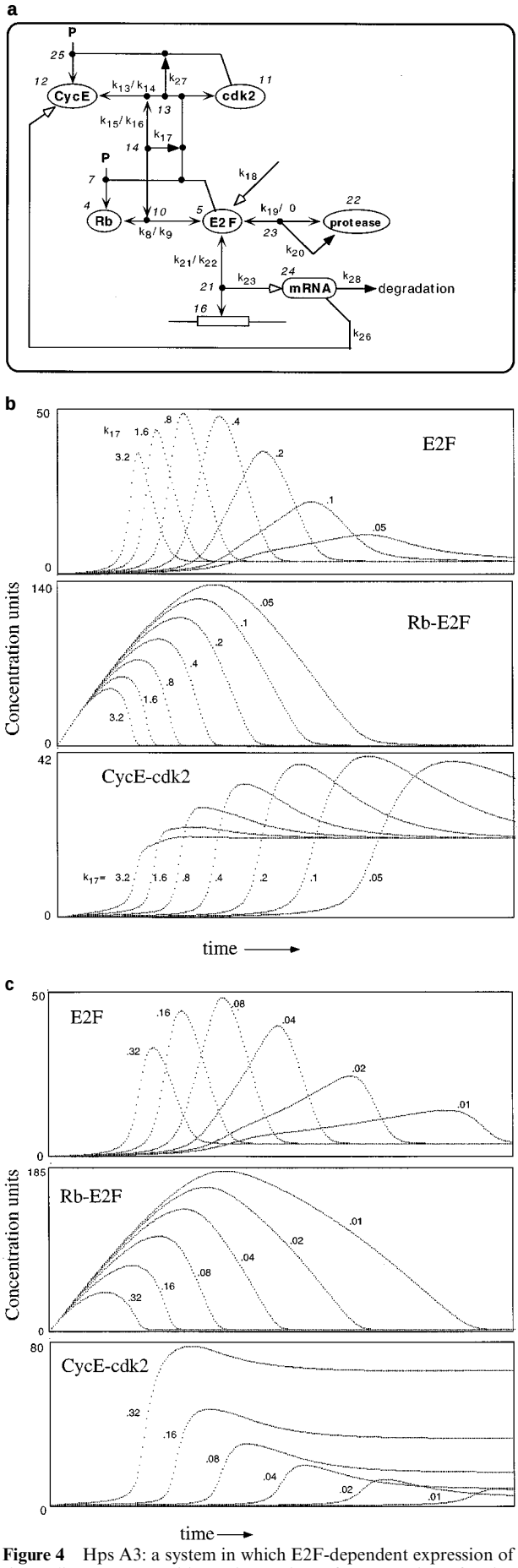


**Figure 4** Hps A3: a system in which E2F-dependent expression of the cyclin E gene provides a sharp trigger for expression of active cyclin E-cdk2. (**a**) Rection diagram. Added to hps A2 are (1) reversible formation of cyclinE-cdk2 heterodimer (species 13) and (2) E2F-dependent expression of the cyclin E gene (species 16). (Note that cyclinE-cdk2 dimer is represented by any filled circle (node) on the double-arrowed line that connects cyclin E and cdk2). CyclinE-cdk2 phosphorylates Rb in Rb-E2F complex; it also autophosphorylates its cyclin E component, thereby removing cyclin E from the system. The phosphorylation of cyclin E entails conversion of cyclinE-cdk2 (species 13) to cyclinE-P (species 25) and cdk2, governed by rate constant $k_{27}$. Cyclin E mRNA (species 24) is transcribed under control of an E2F-promoter complex (species 21, rate constant $k_{23}$); the mRNA is translated with rate constant $k_{26}$ and degraded with rate constant $k_{28}$. (The transcription and translation steps are represented by open arrowheads, because the E2F-promoter complex and the mRNA are not consumed in the reaction (see symbol definitions, Figure 1).) (**b**) Simulation showing the effects of intrinsic activity of cdk2 as reflected by $k_{17}$; $k_{17}$ can be viewed as a surrogate for control of cdk2 by phosphorylation. Parameters: $[cdk2]_o = 200$, [empty E2F elements in promoters of cyclin E genes]$_o = 0.1$, $k_{13} = 0.2$, $k_{14} = 0$, $k_{15} = k_{16} = 0.2$, $k_{21} = k_{22} = 1$, $k_{23} = 16$, $k_{26} = 1.6$, $k_{27} = 0.1$, $k_{28} = 1$ and $k_{17}$ as marked. Other parameters as in hps A2. Horizontal axis runs from 0–96 time units. (**c**) Effects of gene dosage of E2F-regulated cyclin E gene. $k_{17} = 0.4$, [empty E2F elements in promoters of cyclin E genes]$_o$ as marked; other parameters as in **b**

will be seen in hps B, this diminution of E2F response is more striking when cyclinE-cdk2 is allowed to phosphorylate free as well as E2F-bound Rb).

The peak accumulation of Rb-E2F decreases steadily as E2F gene dosage is increased (Figure 4c, middle). The response of cyclinE-cdk2 again shows sharp onset and occur earlier when gene dosage is higher, but this time an earlier response is a larger response (Figure 4c, bottom).

In hps A3, the production of cyclin E is linked to transcription factor E2F, forming a positive feedback loop, and the maximum amount of cyclinE-cdk2 that can form is limited by the fixed total quantity of cdk2. The sharply triggered production of active cyclinE-cdk2 in this model suggests a useful property that could be recruited for additional functions in the evolution of the network. Indeed, cyclin E appears to have essential functions aside from its role in Rb phosphorylation (Ohtsubo *et al*., 1995).

### *Hps A4: cyclinD-cdk4 controls the early expression of active E2F*

In going from hps A3 to hps A4, the cyclinE-cdk2 subsystem is duplicated and modified, yielding what is now called cyclin D and cdk4/6. Both cyclin-cdk pairs can phosphorylate Rb. The essential difference between the two cyclin systems in the present model is that, while cyclin E synthesis is governed by positive feedback from E2F-dependent promoters, cyclin D synthesis occurs in response to external stimuli (Lukas *et al*., 1996 and references cited therein). We model the external stimulus by first-order synthesis and degradation of cyclin D to generate a wave of cyclin D production as indicated in the reaction diagram for hps A4 (Figure 5a). Total cdk4 is constant. The simulation in Figure 5b shows the E2F responses to cyclin D stimuli in the absence of cyclin E. We assume that the cyclin D stimulus will begin after some E2F has accumulated as Rb-E2F; we therefore set $[Rb]_o = 150$ and $[Rb\text{-}E2F]_o = 50$. Although this model produces an E2F response in the absence of cyclin E, the latter may have other essential functions for entry into S phase.

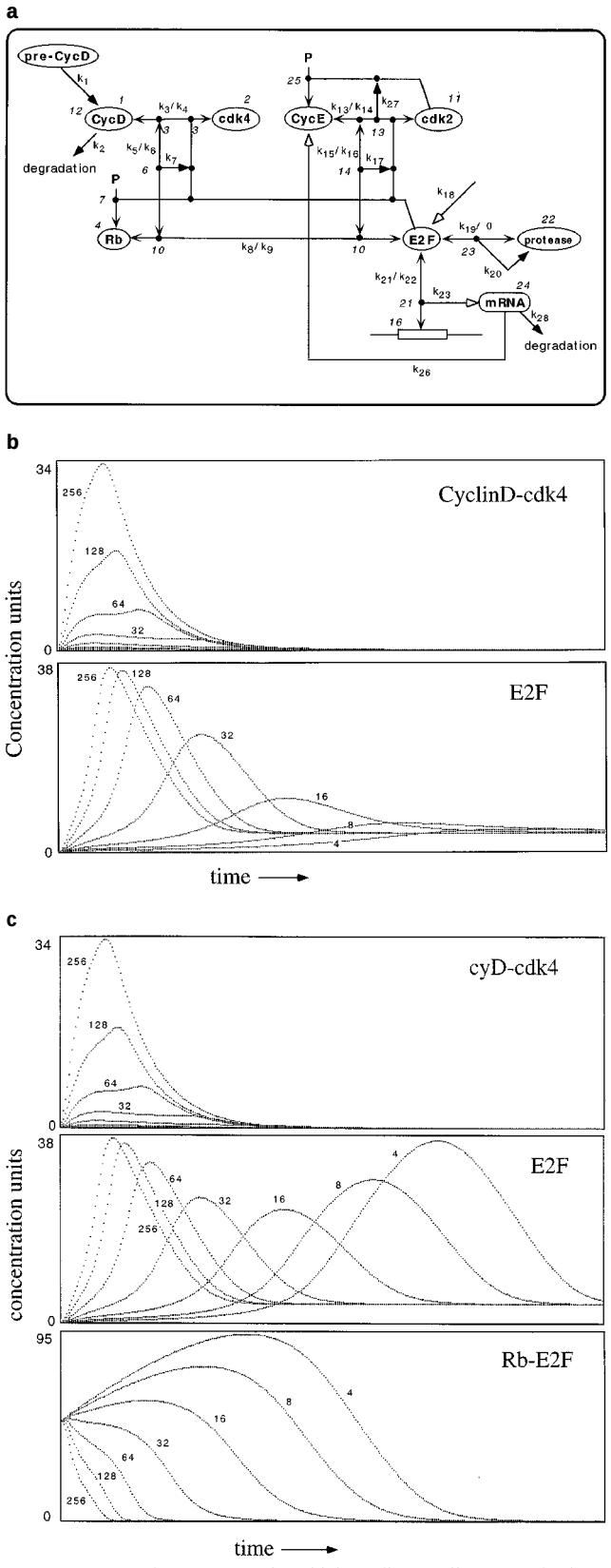


**Figure 5** Hps A4: a system in which cyclin D-cdk4 controls the early expression of active E2F. (**a**) Reaction diagram. Added to hps A3 are cyclin D and cdk4 with Rb phosphorylation reactions parallel to those of cyclinE-cdk2. A wave of cyclin D (external stimulus) is modeled by first-order synthesis and degradation of cyclin D (rate constants $k_1$ and $k_2$), the synthesis occurring by stoichiometric conversion of a 'pre-cyclin D' species to cyclin D. The total cyclin produced (strength of stimulus) equals the initial quantity of pre-cyclin D (since we set $k_1 = 1$). (**b**) Simulations showing E2F responses stimulated by cyclin D in the absence of cyclin E. Size of cyclin D stimulus is determined by the value of [pre-CycD]$_o$. Parameters: $k_1 = k_2 = 1$, $k_3 = 0.01$, $k_4 = 1$, $k_5 = 0.2$, $k_6 = 0$, $k_7 = 4$, $k_{15} = k_{16} = 0$, $k_{17} = 0.4$, [cdk4]$_o = 100$, [Rb]$_o = 150$, [Rb-E2F]$_o = 50$, [pre-CycD]$_o$ as marked. Other parameters as in Figure 4b. Horizontal axis runs from 0–38.4 time units. (**c**) Simulations showing E2F responses stimulated by cyclin D in the presence of cyclin E. $k_{15} = 0.05$, $k_{16} = 0.2$, [pre-CycD]$_o$ as marked. Other parameters as in **b**

E2F responses to cyclin D in the presence of cyclin E and cdk2 are shown in Figure 5c. Even without cyclin D, a large E2F response eventually occurs. What cyclin D does is to preempt the response, causing it to occur earlier, at a time that depends on the cyclin D stimulus strength. Moreover, the amplitude of the response is similar (within a factor of 2 in this set of simulations) for a wide range of cyclin D stimulus strengths.

### *Hps B: A different network sequence supports the generality of the phenomena*

In order to probe the generality of the phenomena and to reveal other features, a second quasi-evolutionary path (hps B) was studied. In contrast to hps A, sequence hps B allows free, as well as E2F-bound, Rb to be phosphorylated by cdk. This difference is important, because the binding of Rb to E2F was made irreversible. In addition, hps B simulations were

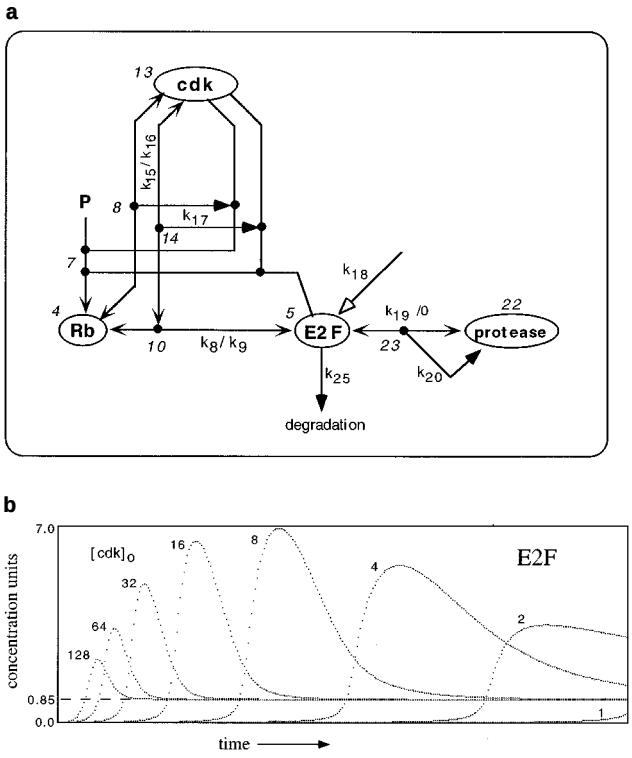


**Figure 6** Hps B2: modification of hps A2 allowing phosphorylation of Rb whether or not it is bound to E2F. (**a**) Reaction diagram. The rate constants for cdk binding to and dissociation from Rb are set equal to the corresponding rate constants for Rb-E2F ($k_{15}$ & $k_{16}$); similarly, the rate constant for phosphorylation ($k_{17}$) is set to be independent of whether Rb is free or bound to E2F. (**b**) E2F responses to the indicated initial concentrations of cdk, showing marked suppression at high [cdk]$_o$. Parameters: $k_8 = 1$, $k_9 = 0$, $k_{15} = 0.1$, $k_{16} = 10$, $k_{17} = k_{18} = 1$, $k_{19} = k_{20} = 2$, $k_{25} = 0.1$, [Rb]$_o = 256$. Horizontal axis runs from 0–160 time units

carried out in a different domain of rate constant settings; in particular, the interaction of Rb-E2F with cdk was skewed heavily towards dissociation.

The reaction diagram for hps B2 (which corresponds to hps A2) is shown in Figure 6a, and a simulation as a function of initial cdk concentration is shown in Figure 6b. The impairment of E2F response at high initial concentrations of cdk was even more striking than it was in the case of hps A2.

The reaction diagram for hps B3 and B4 (which correspond to hps A3 and A4) is shown in Figure 7a. A simulation of hps B3 as a function of E2F gene

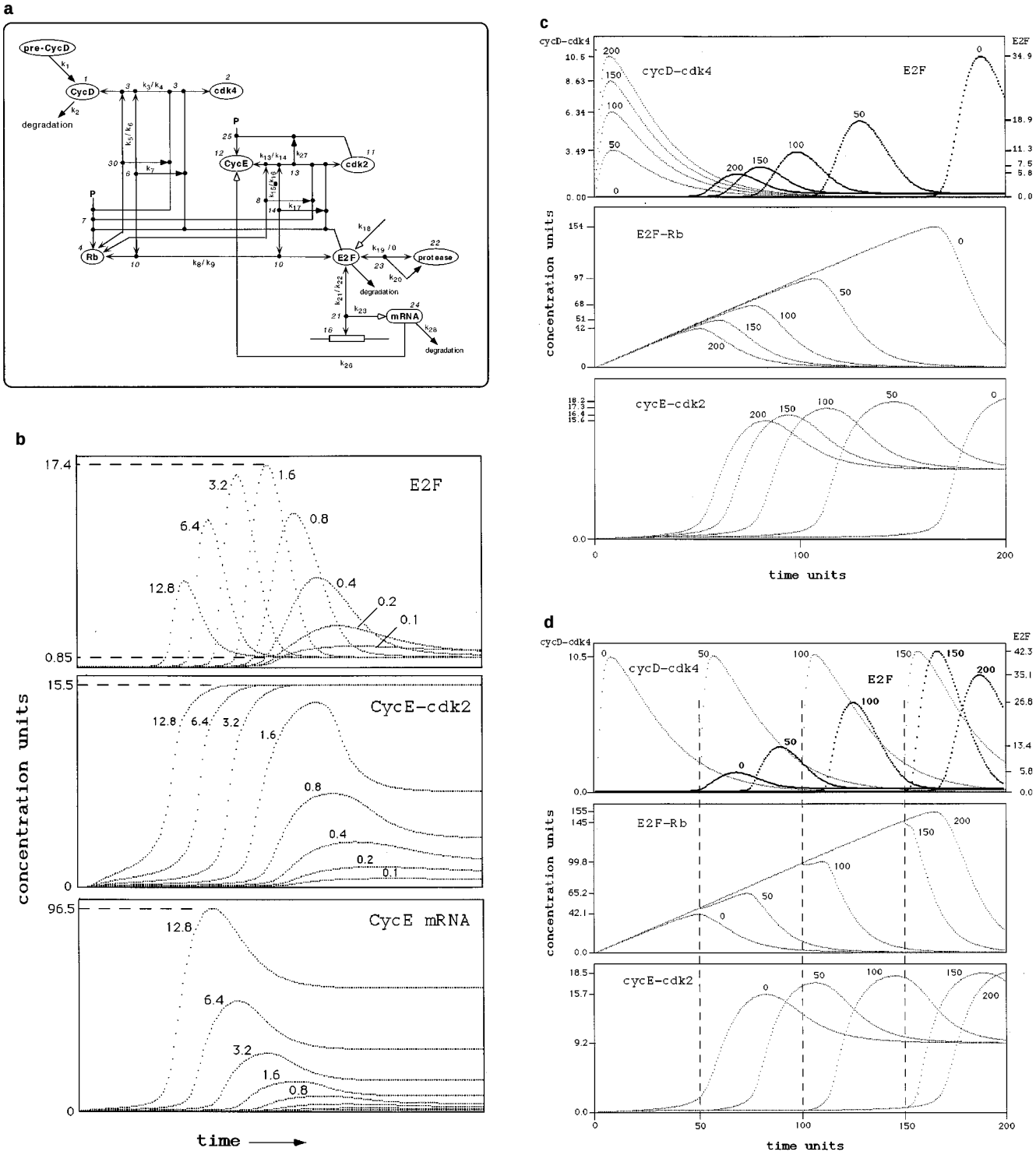


**Figure 7** Hps B3 and hps B4: modification of hps A3 and hps A4 allowing phosphorylation of Rb whether or not it is bound to E2F. (**a**) Reaction diagram of hps B4 (hps B3 is the same without cyclin D and cdk4). The modifications are as explained in the legend of Figure 6a. (**b**) Simulations of hps B3 for the indicated E2F gene dosages. In hps B3, there is no cyclin D stimulus; hence $k_1 = k_2 = k_3 = k_4 = k_5 = k_6 = k_7 = 0$. Parameters: $k_{13} = k_{14} = k_{21} = k_{22} = k_{23} = k_{26} = k_{27} = 1$, $k_{28} = 0.1$, $[Rb]_o = 100$, $[cdk2]_o = 16$, [empty E2F elements in promoters of cyclin E genes]$_o = 0.2$. Other parameters as in Figure 6b. Horizontal axis runs from 0–320 time units. (**c**) Simulations of hps B4 for the indicated cyclin D stimuli. Cyclin D stimulus is gauged by the initial concentration of cyclin D precursor $[pre\text{-}CycD]_o$ as in Figure 5c. Parameters: $k_1 = 0.05$, $k_2 = 4$, $k_3 = 1$, $k_4 = 4$, $k_5 = 0.05$, $k_6 = 10$, $k_7 = 1$, $k_{15} = 0.05$, $[Rb]_o = 200$, $[cdk4]_o = [cdk2]_o = 40$. Other parameters as in (**b**). Time scale runs from 0–200 time units. (**d**) Simulation of hps B4 as function of delay of onset of cyclin D stimulus. Cyclin D production commenced at the indicated times, prior to which Rb-E2F has been accumulating. Cyclin D stimulus = 400. Other parameters as in **c**

dosage is shown in Figure 7b. Despite the monotonic increase in cyclin E mRNA expression, the E2F response diminishes at high E2F gene dosage. The expression of E2F-responsive genes other than the cyclin E gene would therefore be reduced. This suggests that excessive cyclin E gene dosage might under some circumstances impair S phase entry.

The family of curves for cyclinE-cdk2 show a progressively larger and earlier response as cyclin E gene dosage is increased. At large gene dosage, however, cdk2 becomes limiting, and the cyclinE-cdk2 responses become very sharp and shifted in time. This circumstance could be sensitive to changes in available cdk2 due to competition by cyclin A, which accumulates after cyclin E and also binds cdk2.

The response of the network (hps B4) to cyclin D is shown in Figure 7c and d. When the cyclin D stimulus and the production of E2F begin at the same time (Figure 7c), increased stimulus intensity yields earlier, but smaller, E2F responses. When the cyclin D stimulus is delayed for various times after the beginning of E2F production (Figure 7d), the strength of the E2F response in increased (up to the time, about 170 time units, when a response occurs even without cyclin D). This suggests an important role of timing of a proliferation signal relative to the state of the network.

## Discussion

The central idea explored in this work is the notion that useful insights into the functional capabilities of components of complex bioregulatory networks can be obtained by means of a 'quasi-evolutionary' sequence of simulations which progresses by small steps along a path towards increasingly complex networks, in such a manner that each step along the way adds functionality. A quasi-evolutionary path was explored within the network of molecular interactions that are thought to play a role in the G1/S cell cycle phase transition. The model networks were designated 'hypothetical primordial systems' (hps). The starting point of the path was an E2F transcription factor that regulates genes coding for products essential for S phase; E2F was taken to be the output of the system. E2F is a rapidly turning over protein that is degraded by a ubiquitin-dependent proteasome system (Hateboer *et al*., 1996; Hofmann *et al*.,1996); hence we considered E2F to be synthesized at a constant rate and to be degraded by a limited capacity protease. In this system, E2F concentration rises without delay and quickly achieves a steady-state.

Two next steps are readily accessible within the network of known interactions. (1) A protein (corresponding to Rb) could evolve that binds to E2F and inhibits E2F function. (Protein-protein interactions appear to be easy to come by.) (2) E2F, which is already a transcription factor, could function to regulate its own gene; this would merely entail the duplication of already existing E2F elements onto the promoter of the E2F gene. The current study included only (1); a path starting with (2) is under investigation. In the first model (hps A1), Rb was considered to be pre-formed and neither synthesized nor degraded during the cell cycle period being simulated, and Rb was considered to bind rapidly and essentially irreversibly to E2F. The results at this early stage of simplicity are readily predictable: Rb binds most of the E2F being synthesized until Rb becomes nearly saturated with E2F, whereupon free E2F rises to its steady-state governed by synthesis and degradation rates (Figure 2b). An Rb-like factor thus can delay the onset of S phase (which is here assumed to be initiated by production of E2F) and could allow a primordial cell to grow for a period of time before beginning the processes that lead to cell division. In agreement with previous inferences, Herrera *et al*. (1996) recently showed that Rb-deficient embryonic fibroblasts spend less time in G1 and more time in S phase.

The next step along the quasi-evolutionary path is compelling: phosphorylation of Rb with consequent dissociation of the Rb-E2F complex to yield active E2F. This step is carried out by a family of cyclin-dependent kinases (cdk). In hps A2, the effects of cdk (as a single entity of given initial concentration) were determined. Two unexpected, but related, observations emerged. Rb is generally thought of as an inhibitor of E2F transcriptional activity. We found however that the binding and dissociation of E2F by Rb can produce a wave of intense E2F activity (Figure 3b). Rb can store and release E2F in a manner akin to the way a condenser can store and release electric charge. The second and related observation was that excessive cdk activity can deplete Rb before much E2F has been stored, in which case the size of the E2F wave is reduced. It will be interesting to see whether this phenomenon carries over to experimental systems.

The cdk are subject to multiple controls, including (1) cyclins that bind and activate the kinases, (2) stimulatory and inhibitory phosphorylations, and (3) binding of inhibitory molecules. These processes are themselves controlled by other components of the network. A great deal of work will have to be done to characterize the capabilities of all of these connections. The present study set out towards this eventual goal by exploring some of the effects of cyclins. In hps A3, the cyclinE-cdk2 pair was added (Figure 4a). Heterodimer structures, such as cyclinE-cdk2, present an opportunity for two different regulatory modes to impinge on the same activity. Thus cyclin E accumulates as cells enter S phase, while cdk2 remains relatively constant in quantity (although its activity may be altered by phosphorylation). The production of cyclin E was assumed to occur by expression of an E2F-regulated gene, in accord with evidence that the promoter of the cyclin E gene is regulated by E2F (Botz *et al*., 1996). The effect of cdk2 phosphorylation state was mimicked by setting the kinase rate constant ($k_{17}$) to different values (Figure 4b). The effect of cyclin E gene dosage was also examined (Figure 4c). Both cases showed that excessive kinase activity can reduce the size of the E2F wave. The extent of this reduction was limited, however, because only E2F-bound Rb was phosphorylated in this scheme. The effect is much larger when Rb phosphorylation occurs whether or not it is bound to E2F (Figure 6b).

Another finding of interest in hps A3 and B3 was the appearance of sharp transitions in cyclinE-cdk2 (Figures 4b,c and 7b). Perhaps originally evolved as a side-effect, this sharp appearance of kinase activity might later have been utilized in other ways. Indeed, Lukas *et al*. (1997) recently reported that cyclin E (but

not cyclin D1) could force cells into S phase even when the transcriptional activation capability of E2F was suppressed by non-phosphorylatable mutant Rb or by a dominant-negative mutant DP1. Together with previous evidence (reviewed by Bartek *et al.* (1996)), this indicates that cyclin E has other critical targets aside from Rb.

In hps A4, we added cyclin D and its kinase partner cdk4. Simulations showed that expression of cyclin D preempted the E2F response that otherwise occurred at a later time due to the cyclin E circuit (Figure 5c). The combined functions of the two cyclin subsystems therefore could provide a means for timing control of cell proliferation in response to an external signal while maintaining a default proliferative response if no signal arrives within a finite time period.

In a second series, hps B, phosphorylation of Rb was allowed to occur independently of whether the Rb is free or bound to E2F. The impairment of E2F response under conditions of excessive cdk activity was in this case striking (Figures 6b and 7b), and this was also evident for excessive cyclin D stimulus (Figure 7c). The cyclinE-cdk2 response increases with cyclin E gene activity up to a limit determined by available cdk2 whereupon the response acquires a timed switch-like behavior (Figure 7b, middle panel). Since cyclin A and cyclin E could compete for available cdk2, it will be interesting to examine the effects of this additional complexity when cyclin A is added to the system.

E2F production and cyclin D signal are two separate initiating points in the system. E2F production and accumulation as Rb-E2F may occur during G1 phase prior to the arrival of a cyclin D signal. We therefore varied the onset time of the cyclin D signal relative to the start of E2F production (Figure 7d). When a large cyclin D stimulus arrives before much Rb-E2F has accumulated, the E2F response is small; later cyclin D stimuli produce larger E2F responses up to the time when a default response would occur even without cyclin D.

A major finding in this study was that, contrary to current concepts of G1/S phase regulation, acute overexpression of cyclin D-cdk4 or cyclinE-cdk2 activity could under some circumstances inhibit the onset of DNA replication. Seemingly paradoxical effects of cyclin D or E-dependent kinases have been reported. Han *et al.* (1995, 1996) reported that overexpression of cyclin D1 in mammary epithelial cells tends to suppress rather than enhance cell proliferation. In different cell lines, either S or G1 phase was prolonged. The growth inhibition was attributed to overexpression of the cdk inhibitor, $p27^{kip1}$, but other explanations were not excluded, especially because a cyclin D1-overexpressing cell line displayed an increase rather than a decrease in cyclin D1-dependent kinase activity (Han *et al.*, 1996). A similar result was reported with overexpression of cyclin E (Sgambato *et al.*, 1996). Pagano *et al.* (1994) reported that acute overexpression of cyclin D1 with or without concomitant overexpression of cdk4 prevented G1-synchronized cells from entering S phase. These experiments were carried out in serum-starved human embryonic fibroblasts that were microinjected with various expression plasmids. The current simulation studies suggest that coexpression in such experiments of a cdk inhibitor, such as p16 or p21, could prevent the S phase block caused by cyclin D. Pagano *et al.* however attributed the effect of cyclin D1 to an interaction with PCNA and state that 'p21 was not tested [in coexpression with cyclin D1] because alone it inhibits the cyclin-dependent kinases and causes cell cycle arrest.' This illustrates how simulation studies can suggest significant experiments that otherwise might be neglected.

Another finding possibly relevant to these considerations is a recent report by Hua *et al.* (1997) that addition of cyclinE-cdk2 to amphibian egg extracts prevents the DNA replication response that ordinarily is seen when sperm chromatin is added.

The networks in the current study were trimmed to make them as simple as possible while retaining an important functional core. The functional characteristics of several factors that were ignored in the current work remain to be examined in the future. (1) E2F-Rb complexes can bind to E2F promoter elements and function as gene repressors (Johnson *et al.*, 1994). (2) Rb and its family relative, p107, bind to distinct members of the E2F family and regulate different sets of genes (Hurford *et al.*, 1997). (3) E2F regulates the transcription of cyclin A (Schulze *et al.*, 1995). (4) Active E2F requires binding to a DP partner which can be inactivated by cyclinA-cdk2 (Krek *et al.*, 1995). (5) The cdks can bind cdk inhibitors, such as p16 and p21 (reviewed by Sherr and Roberts (1995)). (6) Different sets of Ser and Thr sites on Rb are differentially phosphorylated by cyclin-cdks, which may act in combination to regulate free or E2F-bound Rb (Zarakowska and Mittnacht, 1997). (7) Relocalization between cytoplasm and nucleus may be a significant aspect of regulation. (8) The phosphorylation control of cdks and the role of c-myc are important aspects that remain controversial.

It may be noted that, in the simulations of hps A4 (Figure 5), which were initialized with a pre-existing store of E2F-Rb, the rate constant for phosphorylation of Rb by cyclinD-cdk4 ($k_7$) had to be substantially larger than the corresponding rate constant for cyclinE-cdk2 ($k_{17}$). This is because of the relatively short duration of the cyclin D wave, as opposed to the sustained appearance of cyclin E. It may be of interest to compare the kinetics of these two cyclin-dependent kinase reactions experimentally in defined systems.

A final comment is in order regarding obstacles to meaningful simulations. First, the relevant rate constants are largely unknown. Functional biosystems however are likely to be robust, and could tolerate considerable variation in rate constant values. In the current work, most rate constants were initially set to unity and then subjected to minimum adjustments necessary to yield plausible behavior. Second, the distribution of regulatory molecules within the cell can be grossly non-homogenous. Here again system robustness might save the day. Third, the reaction network is only partially known. Complex systems however must have evolved from simpler primordia, and vestiges of primordial behavior might be discerned at the functional core of modern systems.

## Materials and methods

### *Simulation program*

Simulation of the reaction networks essentially involves the approximate numerical solution of a set of differential

**Table 1** Molecular species file example[a]

| *Species number* | *Initial conc.* | *Species identifiers* |
|---|---|---|
| 1 | 0 | cyD |
| 2 | 100 | cdk4 |
| 3 | 0 | cyD: cdk4 |
| 4 | 150 | Rb |
| 5 | 0 | E2F |
| 6 | 0 | cyD: cdk4: Rb: E2F |
| 7 | 0 | RbP |
| 8 | 0 | not used |
| 9 | 0 | not used |
| 10 | 50 | Rb: E2F |
| 11 | 200 | cdk2 |
| 12 | 0 | cyE |
| 13 | 0 | cyE: cdk2 |
| 14 | 0 | cyE: cdk2: Rb: E2F |
| 15 | 0 | not used |
| 16 | 0.1 | E2F element |
| 17 | 0 | pre-cyD (*variable*)[b] |
| 18 | 0 | pre-Rb |
| 19 | 0 | degrad. product |
| 20 | 1 | pre-E2F |
| 21 | 0 | E2F: E2Felem |
| 22 | 1 | protease |
| 23 | 0 | E2F: protease |
| 24 | 0 | cyEmRNA |
| 25 | 0 | cyE-P |

[a]Corresponds to simulations in Figure 5c. [b]Value set successively to 4, 8, 16, 32, 64, 128, 256 (see Figure 5c)

**Table 2** Reaction file example[a]

| *Rxn*[c] *num* | *Reaction species*[b] | | | *Product species*[b] | | | *Rate const (k)* |
|---|---|---|---|---|---|---|---|
| 1 | 17 | 0 | 0 | 1 | 0 | 0 | 1 |
| 2 | 1 | 0 | 0 | 19 | 0 | 0 | 1 |
| 3 | 1 | 2 | 0 | 3 | 0 | 0 | 0.01 |
| 4 | 3 | 0 | 0 | 1 | 2 | 0 | 1 |
| 5 | 3 | 10 | 0 | 6 | 0 | 0 | 0.2 |
| 6 | 6 | 0 | 0 | 3 | 10 | 0 | 0 |
| 7 | 6 | 0 | 0 | 3 | 5 | 7 | 4 |
| 8 | 4 | 5 | 0 | 10 | 0 | 0 | 0.1 |
| 9 | 10 | 0 | 0 | 4 | 5 | 0 | 0 |
| 10 | −18 | 0 | 0 | 4 | 0 | 0 | 0 |
| 11 | 4 | 0 | 0 | 19 | 0 | 0 | 0 |
| 12 | 12 | 0 | 0 | 19 | 0 | 0 | 0 |
| 13 | 11 | 12 | 0 | 13 | 0 | 0 | 0.2 |
| 14 | 13 | 0 | 0 | 11 | 12 | 0 | 0 |
| 15 | 10 | 13 | 0 | 14 | 0 | 0 | 0.05 |
| 16 | 14 | 0 | 0 | 10 | 13 | 0 | 0.2 |
| 17 | 14 | 0 | 0 | 5 | 7 | 13 | 0.4 |
| 18 | −20 | 0 | 0 | 5 | 0 | 0 | 8 |
| 19 | 5 | 22 | 0 | 23 | 0 | 0 | 4 |
| 20 | 23 | 0 | 0 | 22 | 0 | 0 | 16 |
| 21 | 5 | 16 | 0 | 21 | 0 | 0 | 1 |
| 22 | 21 | 0 | 0 | 5 | 16 | 0 | 1 |
| 23 | −21 | 0 | 0 | 24 | 0 | 0 | 16 |
| 24 | −21 | 0 | 0 | 5 | 0 | 0 | 0 |
| 25 | 5 | 0 | 0 | 19 | 0 | 0 | 0 |
| 26 | −24 | 0 | 0 | 12 | 0 | 0 | 1.6 |
| 27 | 13 | 0 | 0 | 11 | 25 | 0 | 0.1 |
| 28 | 24 | 0 | 0 | 19 | 0 | 0 | 1 |

[a]Corresponds to the reaction diagram in Figure 5a and the simulations in figure 5c. [b]Species numbers are defined in Table 1. [c]Assigned reaction numbers that serve also as subscripts to the rate constants (k)

equations. The procedure used here, however, focuses on the individual reaction steps, each of which corresponds to terms in the differential equations that affect the reactants and products of the particular reaction step. This makes the mathematical representation of the reaction steps more transparent and facilitates successive modification of the network. Moreover, it is not necessary to write out the differential equations explicitly.

Each reaction is represented by up to 3 reactant species, up to 3 product species, and a rate constant. The molecular species are assigned positive integers and initial concentrations, as in Table 1, and the reactions in a network are then assembled in a reaction file, such as in Table 2. The example files in Tables 1 and 2 correspond to the reaction diagram in Figure 5a and in particular to the simulation in Figure 5c. For example, reaction 17 in Table 2 converts reactant species 14 (which can be seen in Table 1 and Figure 5a to correspond to the cyclin E-cdk2-Rb-E2F complex) to product species 5 (E2F), 7 (Rb-P), and 13 (cyclin E-cdk2). This example also illustrates how an enzymatic reaction is represented explicitly as reactants combining to form an enzyme-substrate complex (in this case species 14) which then dissociates to form products which include the regenerated enzyme (the formation and reversal of enzyme-substrate complex are reactions 15 and 16, respectively, and the conversion of enzyme-substrate complex to products is reaction 17). This way of handling enzymatic reactions has the advantages that the Michaelis-Menton steady state approximation is avoided, the reactions are represented in a homogeneous manner, and it is not necessary to write out the differential equations. Each line in the reaction file, in effect, represents the terms in the differential equations that are contributed by that particular reaction; the computer program does the equivalent of executing these terms. The computer program iterates the set of reactions in small time steps, the extent of each reaction being simply the product of the reactant concentrations, the rate constant, and the time step interval. The concentrations of the molecular species are updated after the reaction extents of all the reaction in the network have been determined, so that the results are independent of the order in which the reactions are calculated. For each stoichiometric reaction, the concentration of each reactant is decremented and the concentration of each product species is incremented by the calculated extent of reaction. For non-stoichiometric reactions, one or more of the reactant species are flagged by a minus sign, in which case their concentrations are not decremented. The time step is made small enough to assure that the concentration-*versus*-time curves are nearly independent of the time step interval.

The reaction tables make transparent the pure 'microworld' nature of the models. The advantages of microworld models are discussed by Kholodenko and Westerhoff (1995).

Since there is little information about the values of the rate constants of the reactions, it was necessary to explore various possibilities and to search for plausible behavior. This procedure may not be as problematic as it may first seem, because the control systems should be robust and should function reasonably over a wide range of rate constant settings. Experience with the simulated networks suggested that this was the case in the current studies. In the current studies, the rate constants were generally set initially to unity, and the minimum variations, usually by factors of 2 or 10, were then applied so as to obtain plausible behavior.

A Macintosh disk containing the programs and reaction files that were used to generate the simulations presented in this paper will be provided by the author upon request. (e-mail:kohnk@dc37a.nci.nik.gov or fax: (301)402–0752).

## Abbreviations

hps = hypothetical primordial system, cdk = cyclin-dependent kinase, Rb = retinoblastoma protein.

## Acknowledgements

The author wishes to thank Drs Dmitri S Dimitrov, John N Weinstein, Patrick M O'Connor, Yves Pommier and Martin L Smith for helpful discussions and comments.

## References

Bartek J, Bartkova J and Lukas J. (1996). *Curr. Opin. Cell Biol.*, **6,** 805–814.
Botz J, Zerfass-Thome K, Spitkovsky D, Delius H, Vogt B, Eilers M, Hatzigeorgiou A and Jansen-Durr P. (1996). *Mol. Cell. Biol.*, **16,** 3401–3409.
Campisi J, Medrano EE, Morreo G and Pardee AB. (1982). *Proc. Natl. Acad. Sci. USA*, **79,** 436–440.
DeGregori J, Kowalik T and Nevins JR. (1995). *Mol. Cell. Biol.*, **15,** 4215–4224.
Dou QP, Levin AH, Zhao S and Pardee AB. (1993). *Cancer Res.*, **53,** 1493–1497.
Elledge SJ. (1996). *Science*, **274,** 1664–1672.
Felix M-A, Labbe J-C, Doree M, Hunt T and Karsenti E. (1990). *Nature*, **346,** 379–382.
Fingert HJ, Chang JD and Pardee AB. (1986). *Cancer Res.*, **46,** 2463–2467.
Fingert HJ, Pu AT, Chen ZY, Googe PB, Alley MC and Pardee AB. (1988). *Cancer Res.*, **48,** 4375–4381.
Goldbeter A. (1991). *Proc. Natl. Acad. Sci. USA*, **88,** 9107–9111.
Goldbeter A. (1996). *Biochemical Oscillations and Cellular Rhythms*. Cambridge University Press, New York, NY.
Han EK, Begemann M, Sgambato A, Soh JW, Doki Y, Xing WQ, Liu W and Weinstein IB. (1996). *Cell Growth Differ.*, **7,** 699–710.
Han EK, Sgambato A, Jiang W, Zhang YJ, Santella RM, Doki Y, Cacace AM, Schieren I and Weinstein IB. (1995). *Oncogene*, **10,** 953–961.
Hartwell L and Kastan MB. (1994). *Science*, **266,** 1821–1828.
Hartwell LH and Weinert TA. (1989). *Science*, **246,** 629–643.
Hateboer G, Kerkhoven RM, Shvarts A, Bernards R and Beijersbergen RI. (1996). *Genes & Dev.*, **10,** 2960–2970.
Herrera RE, Sah VP, Williams BO, Makela RP, Weinberg RA and Jacks T. (1996). *Mol. Cell. Biol.*, **16,** 2402–2407.
Hofmann F, Martelli F, Livingston DM and Wang Z. (1996). *Genes & Dev.*, **10,** 2949–2959.
Hua XH, Yan H and Newport J. (1997). *J. Cell Biol.*, **137,** 183–192.
Hurford Jr RK, Cobrinik D, Lee M-H and Dyson N. (1997). *Genes Dev.*, **11,** 1447–1463.
Hutchison CJ, Cox R, Drepaul RS, Gomperts M and Ford CC. (1987). *EMBO J.*, **6,** 2003–2010.
Hyver C and Le Guyader H. (1990). *BioSystems*, **24,** 86–90.
Johnson DG, Ohtani K and Nevins JR. (1994). *Genes & Dev.*, **8,** 1514–1525.
Johnson DG, Schwarz JK, Cress WD and Nevins JR. (1993). *Nature*, **365,** 349–352.
Kauffman S and Willie JJ. (1975). *J. Theor. Biol.*, **55,** 47–93.
Kholodenko BN and Westerhoff HV. (1995). *Trends Biochem. Sci.*, **20,** 52–54.
Kohn KW and Dimitrov DS. (1997). In: *Computer modeling of complex biological systems*. Iyengar SS (ed). CRC Press: Boca Raton, in press.
Krek W, Xu G and Livingston DM. (1995). *Cell*, **83,** 1149–1158.
Lau CC and Pardee AB. (1982). *Proc. Natl. Acad. Sci. USA*, **79,** 2942–2946.
Lock RB. (1992). *Cancer Res.*, **52,** 1817–1822.
Lukas J, Bartkova J and Bartek J. (1996). *Mol. Cell. Biol.*, **16,** 6917–6925.
Lukas J, Herzinger T, Hansen K, Moroni MC, Resnitzky D, Helin K, Reed SI and Bartek J. (1997). *Genes Dev.*, **11,** 1479–1492.
Murray AW. (1992). *Nature*, **359,** 599–604.
Murray AW and Kirschner MW. (1989). *Nature*, **339,** 275–280.
Murray AW, Solomon MJ and Kirschner MW. (1989). *Nature*, **339,** 280–286.
Muschel RJ, Zhang HB, Iliakis G and McKenna WB. (1991). *Cancer Res.*, **51,** 5113–5117.
Nasmyth K. (1993). *Curr. Opin. Cell Biol.*, **5,** 166–179.
Norel R and Agur Z. (1991). *Science*, **251,** 1076–1078.
Novak B and Tyson JJ. (1993a). *J. Theor. Biol.*, **165,** 101–134.
Novak B and Tyson JJ. (1993b). *J. Cell Sci.*, **106,** 1153–1168.
Novak B and Tyson JJ. (1995). *J. Theor. Biol.*, **173,** 283–305.
O'Connor PM. (1997). *Cancer Surveys*, **29,** 151–182.
O'Connor PM, Ferris DK, Hoffmann I, Jackman J, Draetta G and Kohn KW. (1994). *Proc. Natl. Acad. Sci. USA*, **91,** 9480–9484.
O'Connor PM, Ferris DK, Pagano M, Draetta G, Pines J, Hunter T, Longo DL and Kohn KW. (1993). *J. Biol. Chem.*, **268,** 8298–8308.
Obeyesekere MN, Herbert JR and Zimmerman SO. (1995). *Oncogene*, **11,** 1199–1205.
Ohtani K, DeGregori J and Nevins JR. (1995). *Proc. Natl. Acad. Sci. USA*, **92,** 12146–12150.
Ohtsubo M, Theodoras AM, Schumacher J, Roberts JM and Pagano M. (1995). *Mol. Cell. Biol.*, **15,** 2612–2624.
Pagano M, Theodoras AM, Tam SW and Draetta GF. (1994). *Genes Dev.*, **8,** 1627.
Pardee AB. (1988). *UCLA Symp. Mol. Cell. Biol.*, **New Ser 58,** 157–160.
Pardee AB. (1989). *Science*, **246,** 603–608.
Qin XQ, Livingston DM, Ewen M, Sellers WR, Arany Z and Kaelin Jr WG. (1995). *Mol. Cell. Biol.*, **15,** 742–755.
Qin XQ, Livingston DM, Kaelin Jr WG and Adams P. (1994). *Proc. Natl. Acad. Sci. USA*, **91,** 10918–10922.
Rudner AD and Murray AW. (1996). *Curr. Opin. Cell Biol.*, **8,** 773–780.
Schulze A, Zerfass K, Spitkovsky D, Middendorf S, Berges J, Helin K, Jansen-Durr P and Henglein B. (1995). *Proc. Natl. Acad. Sci. USA*, **92,** 11264–11268.
Sgambato A, Han EK, Zhou P, Schieren I and Weinstein IB. (1996). *Cancer Res.*, **56,** 1389–1399.
Sherr CJ. (1996). *Science*, **274,** 1672–1677.
Sherr CJ and Roberts JM. (1995). *Genes & Dev.*, **9,** 1149–1163.
Tobey RA. (1975). *Nature*, **254,** 245–247.
Tyson JJ. (1991). *Proc. Natl. Acad. Sci. USA*, **88,** 7328–7332.
Tyson JJ, Novak B, Chen K and Val J. (1995). *Prog. Cell Cycle Res.*, **1,** 1–8.
Tyson JJ, Novak B, Odell GM, Chen K and Thron CD. (1996). *Trends Biochem. Sci.*, **21,** 89–95.
Wang Q, Fan S, Eastman A, Worland PJ, Sausville EA and O'Connor PM. (1996). *J. Nat. Cancer Inst.*, **88,** 956–963.
Weinberg RA. (1995). *Cell*, **81,** 323–330.
Wells WAE. (1996). *Trends Cell Biol.*, **6,** 228–234.
Won KA and Reed SI. (1996). *EMBO J.*, **15,** 4182–4193.
Zarakowska R and Mittnacht S. (1997). *J. Biol. Chem.*, **272,** 12738–12746.